RESEARCH PAPER

Crystal Structure, Hirshfeld Surface Analysis and Preliminary In Silico Evaluation of 3,3-di(thiophen-2-yl)isobenzofuran-1(3H)-one

B. Balakrishnan[a], Sugumar Paramasivam[b*], S. Vadivel[c], D. Ezhilarasu[d], T. Srinivasan[e]
[a]Department of Physics, P. T. Lee Chengalvaraya Naicker College of Engineering & Technology, Kancheepuram – 631502, Tamil Nadu, India
[b]Department of Physics, Saveetha Engineering College, Saveetha Nagar, Thandalam, Chennai – 603105, Tamil Nadu, India
[c]Department of Physics, C. Abdul Hakeem College of Engineering and Technology, Melvisharam, Ranipet, Tamil Nadu 632509, India
[d]Department of Chemistry, P. T. Lee Chengalvaraya Naicker College of Engineering & Technology, Kanchipuram – 631502, Tamil Nadu, India
[e]Department of Physics, Agurchand Manmull Jain College, Meenambakkam, Chennai – 600061, Tamil Nadu, India
*Corresponding Author: Sugumar Paramasivam, Department of Physics, Saveetha Engineering College, Saveetha Nagar, Thandalam, Chennai – 603105, Tamil Nadu, India
Email: sugumar17283@gmail.com
Received: 20th July 2026; Revised: 11th August 2026; Accepted: 18th September 2026; Available Online: 15th October 2026

ABSTRACT
The present study describes the structural investigation of 3,3-di(thiophen-2-yl)isobenzofuran-1(3H)-one, a thiophene-substituted phthalide derivative. The compound was synthesized and characterized by single-crystal X-ray diffraction to establish its molecular conformation and intermolecular organization in the solid state. The structural analysis indicates a non-planar relationship between the isobenzofuranone core and the thiophene rings, while intermolecular C–H···O contacts contribute to crystal stabilization. Hirshfeld surface analysis and two-dimensional fingerprint plots were employed to quantify the intermolecular contacts governing the packing. The manuscript also presents an in silico workflow involving molecular docking and ADME/drug-likeness assessment; however, the docking target and compound-specific computational results should be verified against the original calculation files before submission because the current draft contains inconsistent target and compound identifiers. Overall, the work provides a structural basis for understanding the conformational and intermolecular features of thiophene-substituted phthalides and supports further investigation of their physicochemical and biological properties.
Keywords: Phthalide; Isobenzofuranone; Thiophene; Single-crystal X-ray diffraction; Hirshfeld surface analysis; Molecular docking; ADMET
How to cite this article: *B. Balakrishnan, Sugumar Paramasivam, S. Vadivel, D. Ezhilarasu, T. Srinivasan. Crystal Structure, Hirshfeld Surface Analysis and Preliminary In Silico Evaluation of 3,3-di(thiophen-2-yl)isobenzofuran-1(3H)-one. Int J Drug Deliv Technol. 2026;16(88s):917-925. DOI: 10.25258/ijddt.16.88s.93.*
Source of support: Nil.
Conflict of interest: None

1. Introduction

Phthalides are a group of secondary metabolites or phytochemical compounds classified under lactones (Ye et al., 2010). Phthalide are known to provide health benefits by stimulating and/or inhibiting various enzymes in the body (Rayabarapu et al., 2004). Studies have shown that these compounds can help lower blood pressure, provide an anti-inflammatory function, improve circulation, rid the body of toxins such as uric acid crystals, inhibit malignancy and offer a calming effect (Bellasio, 1975). Many of the major phthalides have been isolated from plants mainly medicinal herbs, celery stalks, celery seeds and essential oils of their plant of origin (Choi & Sawamura, 2002). There are numerous reports on the bioactivities of phthalides but investigations concerning the mode of action are few. Phthalides (isobenzofuranone), a family of five-membered lactones, are also important building blocks in a large number of biologically active compounds. 3-Arylphthalides, for example, are useful intermediates for the synthesis of tri and tetracyclic natural products such as anthracycline antibiotics (Fei & McDonald, 2007). Phthalides are versatile starting materials for the synthesis of a variety of structures and the derivatives are also key intermediates for the synthesis of natural products (Yang et al., 2003). Some 3- alkyl and 3-aryl substituted phthalides exhibit pharmacological

applications, and some others have been used as starting materials for the synthesis of carbo- and heterocycles. Most of the phthalides were screened for their antimicrobial, analgesic and antioxidant activities. Phthalides exhibit an equally broad spectrum of bioactivity, including modulation of the central nervous system, protection against brain eschemia, modulation of platelet aggregation and cardiac function, inhibition of smooth muscle cell proliferation, anti-angina activity, and smooth muscle relaxation, as well as antibacterial, antifungal, antiviral and phytotoxic activity (Lin et al., 2005).

Recently a series of novel phthalide derivatives were prepared (Purohit Nalini & Yadav, 2012) and the inventors have evaluated the analgesic activity of these compounds. 4,5,6,7-tetrachlorophthalide and its other derivatives are used as effective fungicides. Recently, variation in the fungicide, 4,5,6,7-phthalide, in water was investigated in order to evaluate the runoff of the fungicide after aerial application to paddy fields by a radio-controlled helicopter(Maeda.et al., 2008).

Phthalide derivatives incorporating mono- and di-picolylamino functionalities at the 6-position have been prepared as novel fluoroionophores and their fluorescence responses to metal cations have been investigated. These phthalides not only exhibited efficient fluorescence in an aqueous medium but also displayed fluorescence on–off response upon addition of transition-metal cations, namely Cu2+. The 6-aminophthalide fluorophore served as the core of the fluorescent probes although it has rarely been applied to a chemosensor (Hideki et al., 2011).

Dyes which undergo a change in spectral absorption characteristics in response to a change in pH are well known in the art and are frequently referred to as indicator or pH-sensitive dyes. Typically, these dyes change from one color to another, from colored to colorless or from colorless to colored on the passage from acidity to alkalinity or the reverse and are commonly employed in analytical chemical procedures to measure changes in pH value. Among the indicator dyes most widely used in the group derived from phthalides as exemplified by phenolphthalein, thymolphthalein, o-cresolphthalein and 1-naphtholphthalein.

Novel coloring phthalide compound are prepared and used as recording material capable of yielding images which absorb the light in the near infrared region by thermosensitive recording, pressure-sensitive recording or by use of laser beams. In view of these significant applications, the crystal structures of the Pthalide (isobenzofuranone) derivative has been carried out.

2.1. Experimental

Phthaloyl dichloride (0.6 mL, 4 mmol) and 1.276 g of $AlCl_3$ were mixed thoroughly for 5 min at 0°C. Slowly 1mL (12 mmol) of thiophene in 20 mL of CH_2Cl_2 was added. The mixture was allowed to warm up to room temperature and was stirred for another 30 min. The mixture was poured in 100 mL of ice with 10 mL of HCl (37%). The product was extracted with ether, dried, and purified by column chromatography (n-hexane/$CHCl_3$). Crystallization resulted in white crystals with a yield of 0.71g (60%): mp 100-102 °C.

2.2. Single Crystal X-Ray Diffraction

Single crystal X-ray diffraction data of molecule Isobenzofuran (IBF) was collected on a Bruker Axs Kappa APEXII CCD diffractometer (Bruker, 2008) equipped with a graphite monochromator using ω scan mode. The unit cell parameters were determined from 36 frames measured (0.5° and phi scans) from three different crystallographic zones and using the method of difference vectors. The data reduction and cell refinement were carried out with the help of SAINT (Bruker, 2008) and the structure was solved by direct methods procedure using SHELXS-97 (Sheldrick, 2008) and SIR-92 (Altomare et al., 1993). The normalized structure factors (F) were used for finding the phases. A total of 6476 reflections with E > 1.2 was used for phase refinement procedures. A total of 256 phase sets have been refined of which the set with lowest Combined Figure of Merit (CFOM) was taken as the best set was 0.0711.

2.3. Hirshfeld analysis

The crystallographic details of Isobenzofuran (IBF) compound of the final X-ray refinement at 100 K was used for Hirshfeld surface computations. All the surface analyses calculation was conducted using Crystal Explorer 17.5[Spackman & Jayatilaka, 2009]. The dnorm property was mapped on the generated Hirshfeld surfaces by calculating di and de at each point, normalizing those distances against the respective van der Waals radii of the atoms involved. Red regions in the dnorm map correspond to distances significantly shorter than the sum of the radii, white indicates interactions close to the sum, and blue suggests longer intermolecular separations. Two-dimensional fingerprint plots were subsequently produced to quantify the fraction of the surface involved in each type of contact. This mapping illuminates the extent of hydrogen-bond participation by showing spikes or wings in the fingerprint profiles corresponding to short H···O or other relevant interactions.

2.4. Molecular Docking Modeling

The structure of Ligand Binding domain proteins was retrieved from the Protein Data Bank and all the water molecules and co-crystallized ligands were removed from the downloaded structures (PDBs: 2LBD & 4LBD) [Renaud, et al., 1995; Klaholz, et al., 1998]. The grid box was set for the co-crystallized ligand with dimensions of 20 × 20 × 20 Å (x, y, z) within the LBDs active site. In all docking simulations, the synthesized ligand was flexible and protein remained static conditions. Docked compound interaction diagrams in two dimensional and three dimensional images were generated using Pymol [Lineback & Jansma, 2019]. Docking validation and the binding orientations was carried out using AutoDock [Morris., et al., 2009], and redocking the co-crystallized ligand into the active site region of LBD (2LBD & 4LBD) using the previously set grid box centered on the crystallographic coordinates.

2.5. ADME and physicochemical (drug likeliness) properties

ADME study analyses the chemical behavior of pharmacological compounds in a living organism. All the pharmacokinetic parameters were calculated from the PreADMET online server. This study helps to find out the detailed behavior of compounds by absorption, distribution, metabolism, and excretion in the body. These factors are crucial in drug development and its therapeutic effects and minimizing the side effects. Numerous parameters such as Blood–brain Barrier (BBB), Plasma Protein Binding (PPB), Skin permeability, etc., are used to describe drug toxicity.

Physicochemical parameters help to predict whether a compound has some features to become an effective drug or not. The parameters such as logP, PSA (Polar Surface Area), molecular weight, no. of heavy atoms, etc., were calculated from https://www.molinspiratiom.com. All these parameters are a set of guidelines for Lipinski's rule that assess the drug likeliness of a compound. Any compound with only one violation of Lipinski's rule becomes an orally active drug.

Bioactivity scores, such as those of GPCR ligands, kinase or protease inhibitors, and ion exchange modulators, illustrate the relationship between drugs and receptors. The mol-inspiration online server (https://www.molinspiration.com) helps to calculate the bioactivity score of ligands. Any drug is considered to be active if its bioactivity score is greater than 0.0, moderately active if its score lies between −5.0 and 0.0, and inactive if the score is lesser than −5.0.

3. Results and Discussions

3.1. X-Ray Structural Analysis

The chemical diagram of the Isobenzofuran (IBF) studied and Table 1 summarizes the crystallographic information details for Isobenzofuran (IBF). The corresponding bond lengths and bond angles are presented in Table 2 & 3. The torsion angles for non-hydrogen atoms are listed in Table 4.

Table 1

Summary of crystal data, intensity data collection and refinement details for the **Isobenzofuran (IBF)**

Parameters	Isobenzofuran (IBF)
Chemical formula	$C_{16}H_{10}O_2S_2$
Formula weight	470.54
Temperature	293(2) K
Wavelength	0.71073 Å
Crystal system	Orthorhombic
Space group	P 2121,21
Unit cell dimensions	
a(Å)	7.6180(3)
b(Å)	12.3198(4)
c(Å)	15.0595(5)
α(°)	90
β(°)	90
γ(°)	90
Volume Å^3	1413.37(9)
Z, Calculated density Mg/m^3	4, 1.402
Absorption coefficient mm^{-1}	0.373
F(000)	616
Crystal size mm	0.30 x 0.20 x 0.20
Diffractometer	Bruker Kappa APEXII CCD diffractometer
θ range	2.14to 24.99°
Index ranges	-9≤ h≤ 5
	-14≤ k≤ 14
	-17≤ l≤ 16
Reflections collected / unique	6476 /2422
	[R(int) = 0.0172]
Completeness to theta	99.00%
Refinement method	Full-matrix least-squares on F^2

Data/Restraints / parameters	2422 / 103 / 200
Goodness-of-fit on F^2	1.071
Final R indices [I>2σ(I)]	R1 = 0.0333
	wR2 = 0.0921
R indices (all data)	R1 = 0.0372
	wR2 = 0.0954
Largest diff. peak and hole e.Å^{-3}	0.255 and -0.252

Table 2
Bond lengths (Å) involving non-hydrogen atoms of **Isobenzofuran (IBF)** with esd's in parentheses

Atoms	Angle	Atoms	Angle
C1-C6	1.372(3)	C9-S1	1.713(2)
C1-C2	1.383(3)	C10-C11	1.418(4)
C1-C8	1.516(3)	C11-C12	1.330(5)
C2-C3	1.370(4)	C12-S1	1.691(3)
C3-C4	1.381(4)	C13-C16	1.367(9)
C4-C5	1.367(5)	C13-C16'	1.370(12)
C5-C6	1.395(4)	C13-S2'	1.682(5)
C6-C7	1.458(4)	C13-S2	1.703(3)
C7-O2	1.195(3)	C14-C15	1.318(4)
C7-O1	1.359(3)	C14-C16	1.416(10)
C8-O1	1.467(3)	C14-S2'	1.620(6)
C8-C9	1.502(3)	C15-C16'	1.446(14)
C8-C13	1.504(3)	C15-S2	1.649(4)
C9-C10	1.408(3)		

Table 3
Bond Angels (Å) involving non-hydrogen atoms of **Isobenzofuran (IBF)** with esd's in parentheses

Atoms	Angle	Atoms	Angle
C6-C1-C2	120.8(2)	C11-C12-S1	112.7(2)
C6-C1-C8	108.8(2)	C16-C13-C16'	97.4(7)
C2-C1-C8	130.4(2)	C16-C13-C8	130.8(4)
C3-C2-C1	117.8(2)	C16'-C13-C8	131.7(6)
C2-C3-C4	121.6(3)	C16-C13-S2'	10.8(5)
C5-C4-C3	120.9(3)	C16'-C13-S2'	108.0(6)
C4-C5-C6	117.6(3)	C8-C13-S2'	120.1(2)
C1-C6-C5	121.2(3)	C16-C13-S2	108.2(4)
C1-C6-C7	108.9(2)	C16'-C13-S2	11.0(6)
C5-C6-C7	129.9(2)	C8-C13-S2	120.92(18)
O2-C7-O1	121.1(3)	S2'-C13-S2	118.9(2)
O2-C7-C6	130.7(3)	C15-C14-C16	107.3(4)
O1-C7-C6	108.2(2)	C15-C14-S2'	121.4(3)
O1-C8-C9	108.06(17)	C16-C14-S2'	14.2(4)
O1-C8-C13	106.68(17)	C14-C15-C16'	102.5(5)
C9-C8-C13	113.65(18)	C14-C15-S2	117.1(2)
O1-C8-C1	102.56(17)	C16'-C15-S2	14.7(5)
C9-C8-C1	112.53(19)	C7-O1-C8	111.36(18)
C13-C8-C1	112.46(19)	C12-S1-C9	91.94(14)
C10-C9-C8	127.5(2)	C14-S2'-C13	91.0(3)
C10-C9-S1	111.15(17)	C13-C16'-C15	117.0(9)
C8-C9-S1	121.08(17)	C13-C16-C14	115.6(6)

C9-C10-C11	109.9(2)	C15-S2-C13	91.54(16)
C12-C11-C10	114.2(3)		

Table 4

Torsion angles (°) for the non-hydrogen atoms of **Isobenzofuran (IBF)** with esd's in parantheses

Atoms	Angle	Atoms	Angle
C6-C1-C2-C3	0.2(3)	C13-C8-C9-S1	-36.4(2)
C8-C1-C2-C3	-179.8(2)	C1-C8-C9-S1	-165.68(15)
C1-C2-C3-C4	-0.6(4)	C8-C9-C10-C11	175.0(2)
C2-C3-C4-C5	1.0(4)	S1-C9-C10-C11	0.9(3)
C3-C4-C5-C6	-0.9(5)	C9-C10-C11-C12	-1.1(3)
C2-C1-C6-C5	-0.1(4)	C10-C11-C12-S1	0.9(3)
C8-C1-C6-C5	179.9(2)	O1-C8-C13-C16	-176.6(9)
C2-C1-C6-C7	-178.6(2)	C9-C8-C13-C16	-57.6(9)
C8-C1-C6-C7	1.4(3)	C1-C8-C13-C16	71.8(9)
C4-C5-C6-C1	0.4(4)	O1-C8-C13-C16'	8.3(13)
C4-C5-C6-C7	178.6(3)	C9-C8-C13-C16'	127.2(12)
C1-C6-C7-O2	-179.7(3)	C1-C8-C13-C16'	-103.4(12)
C5-C6-C7-O2	2.0(5)	O1-C8-C13-S2'	-178.4(4)
C1-C6-C7-O1	0.5(3)	C9-C8-C13-S2'	-59.4(4)
C5-C6-C7-O1	-177.8(3)	C1-C8-C13-S2'	70.0(4)
C6-C1-C8-O1	-2.6(2)	O1-C8-C13-S2	5.3(3)
C2-C1-C8-O1	177.4(2)	C9-C8-C13-S2	124.3(2)
C6-C1-C8-C9	-118.4(2)	C1-C8-C13-S2	-106.3(2)
C2-C1-C8-C9	61.5(3)	C16-C14-C15-C16'	2.6(12)
C6-C1-C8-C13	111.6(2)	S2'-C14-C15-C16'	0.4(10)
C2-C1-C8-C13	-68.4(3)	C16-C14-C15-S2	1.0(7)
O1-C8-C9-C10	-91.8(3)	S2'-C14-C15-S2	-1.2(6)
C13-C8-C9-C10	150.0(2)	O2-C7-O1-C8	177.9(3)
C1-C8-C9-C10	20.7(3)	C6-C7-O1-C8	-2.3(3)
O1-C8-C9-S1	81.8(2)	C9-C8-O1-C7	122.0(2)
C13-C8-O1-C7	-115.4(2)	C14-C15-C16'-C13	-2.4(17)
C1-C8-O1-C7	2.9(2)	S2-C15-C16'-C13	172(5)
C11-C12-S1-C9	-0.3(2)	C16'-C13-C16-C14	1.0(14)
C10-C9-S1-C12	-0.4(2)	C8-C13-C16-C14	-175.4(5)
C8-C9-S1-C12	-174.93(19)	S2'-C13-C16-C14	-167(6)
C15-C14-S2'-C13	1.1(6)	S2-C13-C16-C14	2.9(12)
C16-C14-S2'-C13	-8(3)	C15-C14-C16-C13	-2.5(12)
C16-C13-S2'-C14	10(5)	S2'-C14-C16-C13	170(5)
C16'-C13-S2'-C14	-2.3(11)	C14-C15-S2-C13	0.5(3)
C8-C13-S2'-C14	-177.1(3)	C16'-C15-S2-C13	-6(4)
S2-C13-S2'-C14	-0.8(5)	C16-C13-S2-C15	-1.9(7)
C16-C13-C16'-C15	0.9(17)	C16'-C13-S2-C15	8(5)
C8-C13-C16'-C15	177.2(7)	C8-C13-S2-C15	176.6(2)
S2'-C13-C16'-C15	3.2(18)	S2'-C13-S2-C15	0.3(4)
S2-C13-C16'-C15	-170(6)		

Fig 1 shows the ORTEP plot of the molecule drawn at 30% probability displacement ellipsoid with atom numbering scheme. The structure contains a isobenzofuran ring system and two thiophene rings are attached with it. The bond lengths C1 – C8 = 1.516 (3) and C6 - C7 = 1.458(4) Å are slightly deviate from the normal values but are comparable with those of already reported similar structure (Kitamura & Kawase, 2008). In the thiophene ring B, the carbon atom C16 and sulphur

atom S2 are disordered over two sites with occupancy ratio of 0.65(4) : 0.349(4). The isobenzofuran ring system is not strictly planar (the dihedral angle between C1- C6 ring and C1,C8,O1,C7,C6 ring is 1.54(3)°). The isobenzofuran ring system make dihedral angles of 73.4(1)° and 66.6(2)° with the thiophene ring A (C9 – C12/S1) and thiophene ring B (C13 – C16/S2).

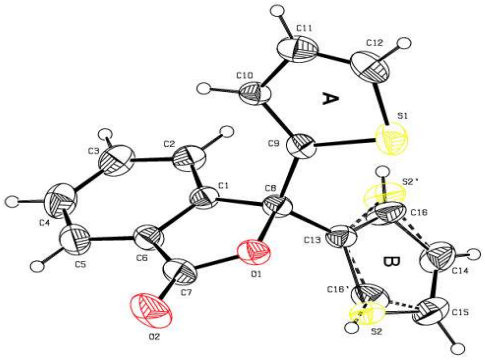


Fig. 1 Thermal Ellipsoid plot of Compound at 30% probability level

3.1.1. Inter and Intra Molecular features

For Compound Isobenzofuran (IBF), the pattern of hydrogen bonding and packing in the crystal are shown in Fig. 2 and 3. The molecular structure is stabilized by intermolecular C--H…O interactions. The oxygen atoms O2 and O1 are involved in C15--H15…O2 and C12--H12…O1 interactions as acceptor atoms. The intermolecular and intramolecular hydrogen bonds are listed in Table 5.

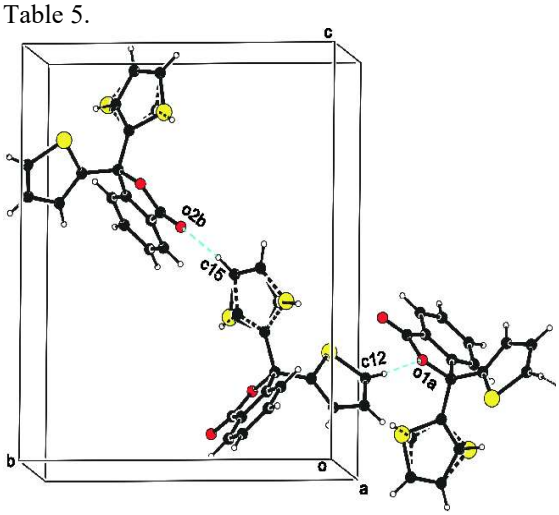


Fig. 2. The Crystal structure of the Compound with C--H…O hydrogen bonding
Scheme shown as dashed lines

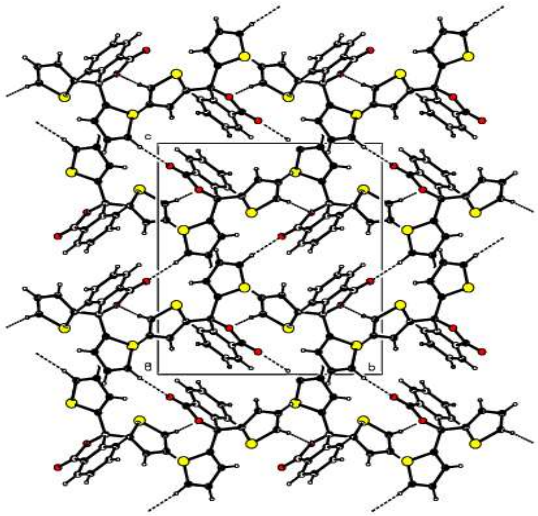


Fig. 3. Packing of the Compound viewed down a-axis

Table 5
Hydrogen bondings and non - bonded interactions [Å and °] for **Isobenzofuran (IBF)**

D-H…A	d(D-H)	d(H …A)	d(D… A)	∠(DH A)
C12 -- H12 ... O1	0.93	2.52	3.43	165
C15 -- H15 … O2	0.93	2.39	3.29	159

Symmetry codes:
(i) 3/2-x, 1-y, 1/2+z
(ii) 2-x, -1/2+y, 1/2-z

3.2. Hirshfeld Surface (HS) Analysis

The dnorm surface and the corresponding 2D fingerprint plots of Isobenzofuran (IBF) are shown in Figs. 4 and 5. In the dnorm map red regions on mark contacts shorter than the sum of van der Waals radii, and the 2D fingerprint plots quantify the relative contribution of each contact type to the surface.

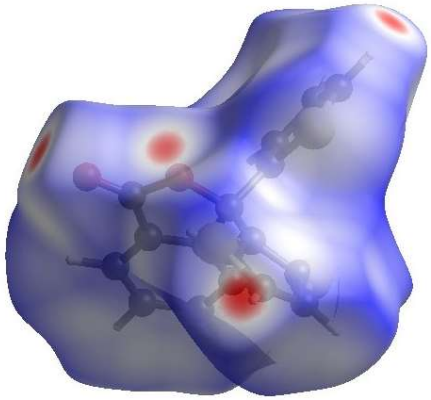


Fig. 4. Hirshfeld surface mapped with d_{norm} for Isobenzofuran (IBF).

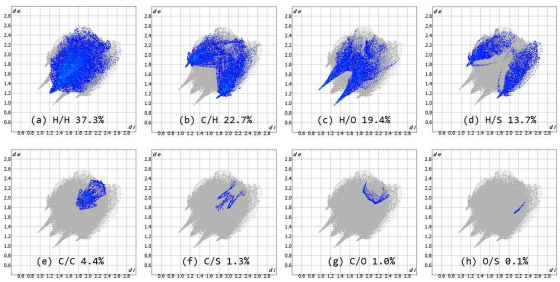


Fig. 5. Two-dimensional fingerprint plots for Isobenzofuran (IBF).

For Isobenzofuran (IBF), the most substantial contributions derive from H···O interactions, accounting for roughly 58.3% of all significant short contacts. This high percentage neatly aligns with the extensive hydrogen-bond network identified in the crystal structure, where N–H···O=C and C–H···O=C motifs form corrugated 2D sheets.

In a Hirshfeld analysis, dominant H···O peaks in the fingerprint plots emphasize the role of hydrogen-bond donors and acceptors in sustaining the crystal lattice. Additionally, the presence of smaller but non-negligible contributions from H···H, H···N, and H···C contacts indicates that weaker dispersion forces and secondary interactions also help stabilize the overall packing arrangement. O···H/H···O interactions (20.7%, 1; 33.9 ± 0.3%, 2), which are the strongest contributors to the individual surfaces. The C–H···π, H···C/C···H contacts (24.9%, 1; 24.9 ± 0.3%, 2), are the second largest contributor to the individual surfaces of 1 and 2. Whereas the H···H contacts (48.5%, 1; 33.7 ± 0.5%, 2) are the largest contribution interactions to the individual surfaces.

3.3. Molecular Docking Analysis of Isobenzofuran (IBF) with Ligand-Binding Domains (2LBD and 4LBD)

Molecular docking studies were performed to investigate the possible binding mode and intermolecular interactions of Isobenzofuran (IBF) within the ligand-binding domains represented by PDB IDs: 2LBD and 4LBD. The docked conformations shown in the figures indicate that IBF can be accommodated within the respective binding pockets and establishes close interactions with key amino acid residues.

Interaction with 2LBD: As illustrated in the first docking image, IBF is positioned within the binding region of the 2LBD protein and exhibits a close interaction with the amino acid residue Thr147 (THR-147). The observed intermolecular contact distance is approximately 2.6 Å, suggesting a favorable polar interaction, potentially involving hydrogen bonding. The orientation of IBF within the binding pocket indicates good spatial complementarity between the ligand and the surrounding amino acid residues, which may contribute to stabilization of the protein–ligand complex.

Interaction with 4LBD: The docking pose of IBF with 4LBD, shown in the second image, reveals multiple close interactions involving Trp46 (TRP-46) and Ser50 (SER-50) residues. The interaction distances observed are approximately 2.7 Å, 1.9 Å, and 2.3 Å, respectively. These short intermolecular distances indicate strong and favorable interactions between IBF and the amino acid residues located within the binding region. In particular, the interaction with the polar SER-50 residue may contribute significantly to stabilization of the docked ligand, while the proximity to TRP-46 may facilitate additional hydrophobic or non-covalent interactions.

Overall, the molecular docking results demonstrate that IBF exhibits favorable binding orientations within both 2LBD and 4LBD, involving key residues such as THR-147, TRP-46, and SER-50. The short interaction distances observed in the docking complexes suggest stable protein–ligand interactions and support the potential binding affinity of IBF toward these ligand-binding domains. Further validation using docking scores, binding free-energy calculations, and molecular dynamics simulations would provide additional insight into the stability and biological relevance of these complexes (Fig. 6).

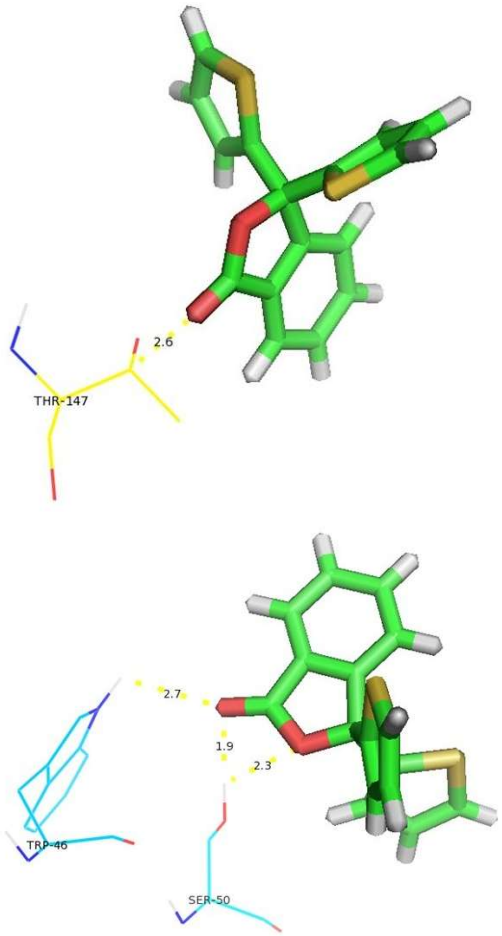


Fig. 6. 2D images of Isobenzofuran (IBF) showing amino acid interactions with target proteins 2LBD (a) and 4LBD (b).

3.4. ADMET Studies.

The likeness of any molecule to be approved as a drug depends greatly on its pharmacokinetic properties as well as its activity. Subsequently, the investigation of the ADMET profile of a molecule should be considered in the early stages of drug design and discovery to avoid the withdrawal possibility of the drug from the pharmaceutical market [Kola & Landis, 2003]. These descriptors identify the absorption, distribution, metabolism, excretion, as well as the toxicity of the examined compound. Although, thereare different invitro experiments that can determine the ADMET profile, in silico determination is an available and reliable tool with the profit of being faster, cheaper, as well as and lifesaver of the experimental animals [Valerio, 2009].

The predicted ADMET profiles of the Isobenzofuran (IBF) that showed correct modes of binding besides Remdesivir, the reference drug, are shown in Fig. 7. Isobenzofuran (IBF) was excluded because of their predicted strong ability to pass the blood-brain barriers which may be combined with a CNS toxicity. Among the excluded compound Isobenzofuran (IBF) was predicted to be inhibitors against the CYP2D6 enzyme which would cause hepatotoxicity. The predicted intestinal absorption and aqueous solubility of all compounds were good to optimal (Fig. 7).

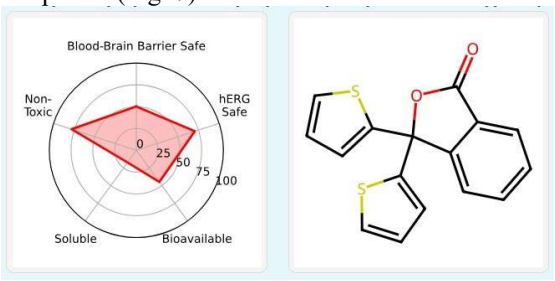


Fig. 7. SwissADME radar charts: ADME profiles of the studied molecules.

4. Conclusions

This study establishes the molecular and crystal structure of 3,3-di(thiophen-2-yl)isobenzofuran-1(3H)-one through single-crystal X-ray diffraction and provides a complementary Hirshfeld surface framework for examining its intermolecular interactions. The molecule consists of a nearly planar isobenzofuranone core with two thiophene rings adopting substantially twisted orientations. Crystal packing is primarily supported by weak C–H···O contacts involving the lactone oxygen atoms. The computational docking and ADME sections provide a preliminary framework for assessing biological relevance; however, the target identity, docking results and quantitative pharmacokinetic descriptors should be verified from the original output files before publication. Overall, the crystallographic results provide a reliable structural foundation for future computational and experimental studies of thiophene-substituted phthalide derivatives.

Declarations

Conflict of Interest: The authors declare no conflict of interest.

Data Availability: Crystallographic and computational data should be made available through the appropriate repository or supplementary material, subject to the authors' data-deposition requirements.

References:

Ye, Z., Lv. G., Wang, W., Zhang, M. & Cheng, J.(2010). Angew. Chem., 122, 3753-3756.

Rayabarapu, D., Chang, H. & Cheng, C. (2004). Chem. Eur. J. 10, 2991-2996.

Bellasio E., German Patent 2422193, 1974; [Chem. Abstr.1975, 83, 9788].

Choi H., Kim M. & Sawamura M. (2002). Constituents of the essential oil of cnidium officinale Makino, a Korean medicinal plant, Flavour Fragr. J. 17, 49 –53.
Fei Z. & McDonald F.E. (2007). Stereo- and Regioselective Glycosylations to the Bis-C-arylglycoside of Kidamycin, Org. Lett., 9, 3547–3550.
Yang, X., Rotter, T., Piazza, C. & Knochel, P. (2003). Org. Lett. 5, 1229-1231 (2003).
Lin, G., Chan, S.-K., Chung, H.-S. & Li, S.-L. (2005). In Studies in Natural Products Chemistry; Rahman, A., Ed.; Elsevier: Amsterdam, Netherlands, pp 611–669.
Purohit Nalini. V & Yadav. P. (2012). Research Journal of Chemical Sciences, Vol. 2(8), 57-61.
Maeda, T., Iwashita, M., Hori, T., Asada, T., Oikawa, K. & Kawata, K. (2008). Bull Environ Contam Toxicol. 80(5). 399-402.
Hideki, O., Ayako, M. & Kyosuke, S. (2011). Analyst, 136, 3164.
Bruker (2008). APEX2, SAINT and SADABS. Bruker AXS Inc., Madison, Wisconsin, USA.
Sheldrick, G. M. (2008). Acta Cryst. A64, 112–122.
Altomare, A., Cascarano, G., Giacovazzo, C. & Guagliardi, A. (1993). J. Appl. Cryst. 26, 343–350.
Spackman, M. A.; Jayatilaka, D. Hirshfeld surface analysis. CrystEngComm 2009, 11, 19–32.
Renaud, J.P., Rochel, N., Ruff, M., Vivat, V., Chambon, P., Gronemeyer, H., Moras, D. (1995), Crystal structure of the RAR-gamma ligand-binding domain bound to all-trans retinoic acid. Nature 378: 681-689
Klaholz, B.P., Renaud, J.P., Mitschler, A., Zusi, C., Chambon, P., Gronemeyer, H., Moras, D. (1998), Conformational adaptation of agonists to the human nuclear receptor RAR gamma. Nat Struct Biol 5: 199-202
Lineback JE, Jansma AL. PyMOL as an instructional tool to represent and manipulate the myoglobin/hemoglobin protein system. J Chem Educ.2019; 96: 2540–4.
Morris GM, Huey R, Lindstrom W, Sanner MF, Belew RK, Goodsell DS, et al. AutoDock4 and AutoDockTools4: Automated docking with selective receptor flexibility. J Comput Chem. 2009;30(16):2785–91.
https://doi.org/10.1002/jcc.21256 PMID: 19399780
Kitamura, C. & Kawase, T. (2008). Acta Cryst. E64, o1696.
Kola, I.; Landis, J. Can the pharmaceutical industry reduce attrition rates? Nature Reviews Drug Discovery 2004, 3, 711–715. https://doi.org/10.1038/nrd1470
Valerio, L. G., Jr. In silico toxicology for the pharmaceutical sciences. Toxicology and Applied Pharmacology 2009, 241, 356–370. https://doi.org/10.1016/j.taap.2009.08.022